MASTER

Time-Optimal Design and Control of Electric Race Cars Equipped with Multi-Speed Transmissions

Cartignij, C.J.G.

Award date:
2022

EINDHOVEN UNIVERSITY OF TECHNOLOGY

MASTER THESIS

Time-Optimal Design and Control of Electric Race Cars Equipped with Multi-Speed Transmissions

Master	Mechanical Engineering
Department	Mechanical Engineering
Research group	Control Systems Technology

Author	*Student numbers*
Cartignij, C.J.G.	1014018

Supervisor
dr. ir. M.R.U. Salazar Villalon

Eindhoven, December 9, 2022

Time-Optimal Design and Control of Electric Race Cars Equipped with Multi-Speed Transmissions

Camiel Cartignij

Abstract—This thesis presents models and algorithms to jointly optimize the design and control of an electric race car equipped with a multiple-gear transmission (MGT), specifically accounting for the discrete gearshift dynamics. To benchmark its performance, we also consider other transmission types, namely a fixed-gear transmission (FGT) and a continuously variable transmission (CVT). First, we develop convex models for the vehicle dynamics, the FGT, the CVT, the electric motor (EM), the inverter, and the battery, and we develop a mixed-integer model for the MGT. Second, we devise a computationally efficient algorithm to optimize the design and control of an MGT-equipped car, including the gear ratio design, the gearshift trajectory, and the EM power trajectory. In particular, we develop an iterative algorithm, which combines convex optimization and Pontryagin's Minimum Principle to solve the mixed-integer optimization problem. Third, we showcase our algorithm by comparing the performance of a race car equipped with an FGT, a CVT and an MGT with 2 to 4 speeds on the Zandvoort race track. Our results show that the shortest lap time is obtained by the 3-speed MGT-car, because it combines a high powertrain efficiency with fast acceleration, in exchange for a limited increase in weight. Finally, we leverage the computational efficiency of our algorithm to evaluate the influence of the EM size and battery energy limit on the achievable lap time, which reveals that an MGT with 2 or 3 speeds is best suited for most scenarios.

I. INTRODUCTION

THE electrification of automotive powertrains has sparked significant attention over the last years. Conventional passenger vehicles are being replaced by hybrid and fully electric vehicles [1], while existing racing classes are also hybridized, and new fully electric racing classes are emerging. In motorsport, every millisecond counts, so all involved technologies are pushed to their limits. For electric racing, the available battery energy is a significant limitation, which means that optimal energy management and electric motor (EM) efficiency can make the difference to win a race. To extract maximum performance while keeping the EM within its most efficient operating range, various transmission types can be used, which yield control over the EM operating range, at the cost of the transmission's own efficiency and weight. At one end of the spectrum, the fixed-gear transmission (FGT) is light and efficient, while providing little control over the operating range of the EM. At the other end, the continuously variable transmission (CVT) provides continuous control over the EM operation, at the cost of increased weight and decreased efficiency. Between these extremes, the multiple-gear transmission (MGT) balances the efficiency of an FGT with the operating range control of a CVT. To select the optimal transmission for any given application, a joint optimization of transmission design and powertrain control
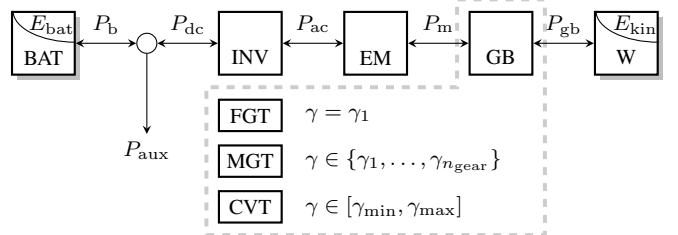

Fig. 1. Schematic layout of the electric race car powertrain under consideration, consisting of a battery (BAT), an inverter (INV), an electric motor (EM), a transmission (GB) and the wheels (W). The arrows indicate power flows between components.

is required. However, the gearshifts of an MGT introduce discrete dynamics, which turns the optimization of an MGT-equipped race car into a mixed-integer optimal control problem (MIOCP). MIOCPs are generally $\mathcal{NP}$-hard, and can be very difficult to solve [2]. Against this backdrop, this thesis presents a computationally efficient algorithm for the optimization of the design and control of an MGT-equipped electric race car.

Related literature: The mixed-integer time-optimal design and control problem studied in this thesis pertains to two main research streams, namely, energy management and time-optimal control of (hybrid) electric vehicles.

For energy management, mainly non-causal optimization is applied on drive cycles with known velocity and torque requirements. Gearshift strategies for an MGT have been optimized using dynamic programming [3], Pontryagin's Minimum Principle (PMP) [4] and iterative combinations of dynamic programming, PMP and convex optimization [5]–[9]. In [10], [11] the authors use outer convexification and rounding to efficiently solve the gearshift problem, while others use brute-force mixed-integer programming [4] and derivative-free methods [12], [13]. Joint optimization of the gearshift strategy and gear ratio design has been done using dynamic programming [14], combined dynamic programming and convex optimization [5] and mixed-integer nonlinear optimization [15]–[17]. For the design and control of an FGT and CVT, [18] applies analytic optimization, while [5], [19] use convex optimization, with [20] also considering a thermal EM model. However, since these methods use known drive cycles, none of them can be directly applied to time-optimal control problems, where the velocity trajectory is unknown.

For the time-optimal control of race cars, [21] proposes a distance-based convex optimization framework. This framework is extended to consider the design and control of an FGT

and CVT by [22], while [23] includes a thermal EM model, and [24] adds modeling of tyre grip limits, and optimization of the FGT ratios for individual tyres. In [25], the MGT gearshift is optimized by using iterative dynamic programming with PMP and convex optimization, while [26] uses outer convexification and nonlinear programming to optimize the gearshift. However, to the best of the authors' knowledge, there are no frameworks for time-optimal control of race cars considering the gearshifts as well as the gear ratio design.

Statement of Contributions: This thesis provides a computationally efficient framework to optimize the design and control of the electric race car shown in Fig. 1, considering an FGT, an MGT and a CVT. We optimize the FGT- and CVT-equipped cars by employing convex optimization, and we introduce an efficient iterative algorithm to optimize the MGT-equipped car, by combining convex optimization with PMP to efficiently account for the discrete gearshift dynamics. Finally, we leverage our algorithm's efficiency to compare the performance of a race car equipped with an FGT, a CVT and 2- to 4-speed MGTs on the Zandvoort race track for multiple battery energy limits and EM sizes.

Organization: The remainder of this thesis is structured as follows: Section II presents a convex model of the powertrain, whilst Section III describes the iterative algorithm for MGT optimization. In Section IV we showcase the results obtained with our algorithm, together with a validation of the algorithm's performance. In Section V we draw the conclusions and provide an outlook on future research.

II. MODELING AND PROBLEM DEFINITION

In this section, we define the minimum-lap-time design and control problem for the powertrain shown schematically in Fig. 1. Our problem is fully convex, except for the mixed-integer gear selection of the MGT. We formulate our problem by extending the framework developed in [22] for FGT and CVT optimization. We add the MGT model, and improve upon the accuracy of the EM and CVT loss models. Furthermore, we include the more accurate vehicle and inverter models from [27]. In this framework, we consider the EM to be the limiting factor with respect to speed, torque and power, so we do not consider any of these limitations for the battery, inverter or transmission models.

A. Objective and State Dynamics

We construct the minimum-lap-time design and control problem in space-domain, which grants us a finite horizon, and enables us to easily implement position-dependent parameters such as the road slope and corner radius. The objective is to minimize the lap time T, given by

$$\min T = \min \int_0^S \frac{\mathrm{d}t}{\mathrm{d}s}(s)\mathrm{d}s,$$

where S is the track length and $\frac{\mathrm{d}t}{\mathrm{d}s}(s)$ is the lethargy, or the inverse of the velocity. As Fig. 1 shows, our model contains two state variables: the battery energy $E_{\mathrm{bat}}(s)$ and

the kinetic energy $E_{\mathrm{kin}}(s)$. We define the battery energy with the integrator

$$\frac{\mathrm{d}E_{\mathrm{bat}}(s)}{\mathrm{d}s} = -F_{\mathrm{i}}(s), \tag{1}$$

where $F_{\mathrm{i}}(s)$ is the internal battery force, the space-derivative of the battery energy. We assume that the battery does not exceed its energy limits during the lap, so we only constrain ΔE_{bat}, the maximum energy consumption over a lap, with

$$E_{\mathrm{bat}}(0) - E_{\mathrm{bat}}(S) \leq \Delta E_{\mathrm{bat}}. \tag{2}$$

At the wheel-side of the vehicle model, we define the kinetic energy integrator using the longitudinal vehicle dynamics assuming steady-state cornering, through

$$\frac{\mathrm{d}E_{\mathrm{kin}}(s)}{\mathrm{d}s} = F_{\mathrm{x,F}}(s) + F_{\mathrm{x,R}}(s) - F_{\mathrm{drag}}(s) - F_{\mathrm{g}}(s), \tag{3}$$

where $F_{\mathrm{x},j}(s)$ denotes the longitudinal force at axle j, with $j \in \{\mathrm{F},\mathrm{R}\}$ denoting the front and rear axle, respectively. Furthermore, $F_{\mathrm{drag}}(s)$ is the aerodynamic drag, and $F_{\mathrm{g}}(s)$ is the gravitational drag. Since we are optimizing over a single lap, we constrain the kinetic energy at the beginning and end of the lap to be equal, using

$$E_{\mathrm{kin}}(0) = E_{\mathrm{kin}}(S). \tag{4}$$

In order to connect the state variables to the objective function in a convex fashion, we define

$$E_{\mathrm{kin}}(s) \geq \frac{1}{2} \cdot m_{\mathrm{tot}} \cdot v(s)^2, \tag{5}$$

where m_{tot} is the total vehicle mass, and $v(s)$ is the vehicle velocity, related to the lethargy through

$$\frac{\mathrm{d}t}{\mathrm{d}s}(s) \cdot v(s) \geq 1. \tag{6}$$

We relaxed the equality signs in (5) and (6) to inequalities, which allows us to convert each equation into a convex second-order cone constraint (SOCC), as described in Appendix A. Since the objective is to minimize the lethargy, these constraints should be active at the optimal solution.

In order to properly compare the various transmission types, we consider the total vehicle mass as

$$m_{\mathrm{tot}} = \begin{cases} m_0 + m_{\mathrm{m}} + m_{\mathrm{cvt}} & \text{if CVT,} \\ m_0 + m_{\mathrm{m}} + m_{\mathrm{gb0}} + m_{\mathrm{gear}} \cdot n_{\mathrm{gear}} & \text{if FGT, MGT,} \end{cases} \tag{7}$$

where m_0 is the base mass of the vehicle without transmission or EM, m_{m} is the EM mass, m_{cvt} is the CVT mass, m_{gb0} is the mass of a geared transmission without gears, and m_{gear} is the mass of a single FGT or MGT gear. To evaluate the effect of the EM size, we scale the mass of the EM linearly, as

$$m_{\mathrm{m}} = m_{\mathrm{m0}} \cdot s_{\mathrm{m}}, \tag{8}$$

where s_{m} is the scaling factor, and m_{m0} is the mass of the unscaled EM.

B. Vehicle Dynamics

In this section, we introduce a model for the vehicle dynamics by reformulating the bicycle model developed in [27]. This allows us to impose limits on the vehicle velocity and propulsive force based on the road slope and corner radius. First, we describe the longitudinal forces acting on the vehicle, defining the aerodynamic drag force as

$$F_{\text{drag}}(s) = \frac{\rho \cdot c_{\text{d}} \cdot A_{\text{f}}}{m_{\text{tot}}} \cdot E_{\text{kin}}(s), \tag{9}$$

where ρ is the air density, c_{d} is the drag coefficient, and A_{f} is the frontal area of the vehicle. Second, we define the gravitational drag as

$$F_{\text{g}}(s) = m_{\text{tot}} \cdot g \cdot \sin(\theta(s)), \tag{10}$$

where g is the gravitational constant and $\theta(s)$ is the road inclination. Lastly, we define the longitudinal axle force as

$$F_{\text{x},j}(s) = F_{\text{gb},j}(s) - c_{\text{r},j} \cdot F_{\text{z},j}(s) - F_{\text{brk},j}(s), \tag{11}$$

where $F_{\text{gb},j}(s)$ is the gearbox output force at axle j, $c_{\text{r},j}$ is the rolling resistance coefficient, $F_{\text{z},j}(s)$ is the vertical axle force, and $F_{\text{brk},j}(s)$ is the brake force per axle, which is defined to be non-negative,

$$F_{\text{brk},j} \geq 0, \tag{12}$$

with a fixed brake balance r_{brk} between the axles,

$$F_{\text{brk,F}}(s) \cdot r_{\text{brk}} = F_{\text{brk,R}}(s) \cdot (1 - r_{\text{brk}}). \tag{13}$$

The total vertical force pushing on the vehicle consists of its weight and aerodynamic downforce $F_{\text{down}}(s)$, described by

$$F_{\text{z,F}}(s) + F_{\text{z,R}}(s) = m \cdot g \cdot \cos(\theta(s)) + F_{\text{down}}(s), \tag{14}$$

where the downforce is defined as

$$F_{\text{down}}(s) = \frac{\rho \cdot c_{\text{l}} \cdot A_{\text{f}}}{m_{\text{tot}}} \cdot E_{\text{kin}}(s), \tag{15}$$

with lift coefficient c_{l}. The maximum longitudinal and lateral forces on axle j are constrained by the tyre grip limits with

$$(F_{\text{z},j}(s) \cdot \mu_j)^2 \geq F_{\text{x},j}^2(s) + F_{\text{y},j}^2(s), \tag{16}$$

where μ_j is the tyre friction coefficient and $F_{\text{y},j}(s)$ is the lateral axle force. The total lateral force acting on the vehicle is defined by the lateral force balance,

$$F_{\text{y,F}}(s) + F_{\text{y,R}}(s) = \frac{2 \cdot E_{\text{kin}}(s)}{R_{\text{track}}(s)}, \tag{17}$$

where $R_{\text{track}}(s)$ is the space-dependent track radius. By assuming steady-state cornering, i.e., no yaw moment, the lateral tyre force balance can be defined as

$$F_{\text{y,F}}(s) \cdot l_{\text{F}} = F_{\text{y,R}}(s) \cdot l_{\text{R}}, \tag{18}$$

where l_{F} and l_{R} represent the longitudinal distance between the center of gravity and the front and rear axle, respectively. Lastly, we define the longitudinal force balance using the pitch moment equilibrium as

$$F_{\text{z,R}} \cdot l_{\text{R}} + F_{\text{down}} \cdot l_{\text{gp}} = (F_{\text{x,F}} + F_{\text{x,R}}) \cdot h_{\text{g}} \\ + F_{\text{z,F}} \cdot l_{\text{F}} + F_{\text{drag}} \cdot h_{\text{gp}}, \tag{19}$$

where h_{g} is the height of the center of gravity with respect to the tyre contact patch, and h_{gp} and l_{gp} are the vertical and longitudinal distance, respectively, between the center of gravity and the center of pressure of the vehicle.

C. Transmission

In this section, we present constraints for the gear ratio and models for the losses of the FGT, MGT and CVT. For the sake of notational simplicity we include ratios and losses for the final drive directly in the component models. Henceforth, we will consider a rear-wheel driven vehicle, so we set $F_{\text{gb,F}}(s) = 0$, and for notational convenience $F_{\text{gb}}(s) = F_{\text{gb,R}}(s)$. Since the FGT and MGT technologies have a relatively constant efficiency [28], we consider their losses using the constant efficiencies η_{fgt} and η_{mgt}, respectively, using the convex notation from [22],

$$F_{\text{gb}}(s) \leq \begin{cases} \eta_j \cdot F_{\text{m}}(s) \\ \dfrac{1}{\eta_j} \cdot F_{\text{m}}(s) \end{cases} \quad j \in \{\text{fgt, mgt}\}, \tag{20}$$

where $F_{\text{m}}(s)$ represents the mechanical EM force. The gear ratio $\gamma(s)$ of the FGT is defined as

$$\gamma(s) = \gamma_1, \tag{21}$$

with γ_1 being the ratio of its first and only gear. For the MGT, we introduce the binary gearshift variable $b(s) \in \mathbb{B}^{n_{\text{gear}}} = \{0,1\}^{n_{\text{gear}}}$, which allows us to write the active gear ratio as

$$\gamma(s) = \sum_{i=1}^{n_{\text{gear}}} \gamma_i \cdot b_i(s), \tag{22}$$

where n_{gear} is the number of gears. To make sure only one gear is active simultaneously, we define

$$\sum_{i=1}^{n_{\text{gear}}} b_i(s) = 1.$$

Similar to [25], we assume that gearshifts occur instantaneously and without shifting losses, since we consider a high-performance quick-shift transmission.

For the CVT, the gear ratio is fixed to lay within the range

$$\gamma(s) \in [\gamma_{\text{min}}, \gamma_{\text{max}}], \tag{23}$$

where the limits are defined by a constant ratio coverage c_γ,

$$\gamma_{\text{min}} = c_\gamma \cdot \gamma_{\text{max}}. \tag{24}$$

Since the CVT is strongly characterized by its efficiency, we employ an enhanced form of the transmission loss model proposed in [22]. We approximate the gearbox losses with a quadratic model,

$$P_{\text{m}}(s) - P_{\text{gb}}(s) = x_{\text{gb}}^\top(s) Q_{\text{gb}} x_{\text{gb}}(s),$$

with $Q_{\text{gb}} \in \mathbb{S}_+^5$, where $\mathbb{S}_+^j$ describes a $j \times j$ symmetric positive semi-definite matrix. We define $x_{\text{gb}}(s)$ as a vector containing the in- and outputs of the CVT, given by

$$x_{\text{gb}}(s) = \begin{bmatrix} \dfrac{1}{\sqrt{\omega_{\text{m}}(s)}} & \sqrt{\omega_{\text{m}}(s)} & \dfrac{\omega_{\text{gb}}(s)}{\sqrt{\omega_{\text{m}}(s)}} & \dfrac{P_{\text{m}}(s)}{\sqrt{\omega_{\text{m}}(s)}} & \dfrac{P_{\text{gb}}(s)}{\sqrt{\omega_{\text{m}}(s)}} \end{bmatrix}^\top,$$
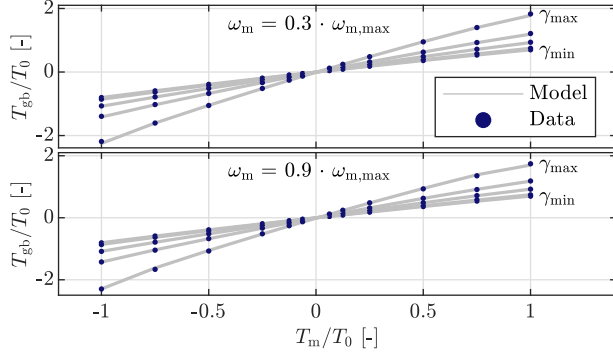
Fig. 2. Comparison between the gearbox output torque (T_{gb}) of the measured data and the convex model of the CVT for various gear ratios at two different input speeds. The normalized RMSE of the output power of the full model is 0.38 %.
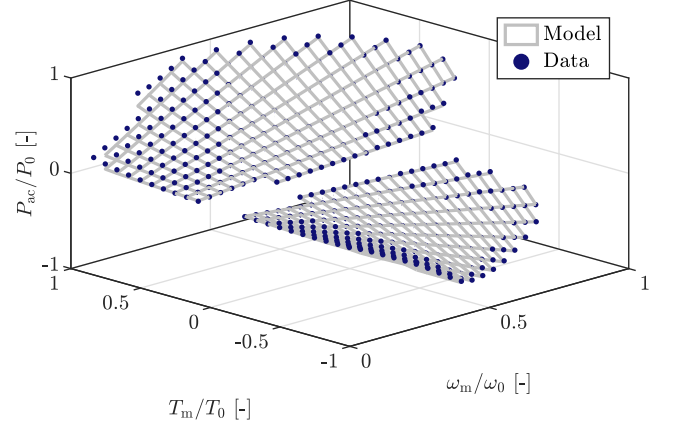

Fig. 3. Normalized comparison between the EM input data and model. The normalized RMSE of the input power is 0.94 %.

where $\omega_{\text{m}}(s)$ and $\omega_{\text{gb}}(s)$ are the EM and CVT output speed, and $P_{\text{m}}(s)$ and $P_{\text{gb}}(s)$ are the EM and CVT output power, respectively. We determine the fitting coefficients of the Q_{gb} matrix using semi-definite programming. Since the model estimates the CVT losses, while both $P_{\text{gb}}(s)$ and $P_{\text{m}}(s)$ are present in $x_{\text{gb}}(s)$, a very accurate fit can be obtained, as shown in Fig. 2. Finally, we convert the power-based loss model to forces by multiplying with the lethargy-squared, yielding

$$(F_{\text{m}}(s) - F_{\text{gb}}(s)) \cdot \frac{\gamma(s)}{r_{\text{w}}} \geq y_{\text{gb}}(s)^{\top} Q_{\text{gb}} y_{\text{gb}}(s), \qquad (25)$$

where r_{w} is the wheel radius, and with

$$y_{\text{gb}}(s) = \begin{bmatrix} \frac{\mathrm{d}t}{\mathrm{d}s}(s) & \frac{\gamma(s)}{r_{\text{w}}} & \frac{1}{r_{\text{w}}} & F_{\text{m}}(s) & F_{\text{gb}}(s) \end{bmatrix}^{\top}. \qquad (26)$$

Since Q_{gb} is a positive definite matrix, this model can be converted into an SOCC, as shown in Appendix A.

D. Electric Motor

In this section, we derive a scalable model of the EM. We provide a convex loss model, together with convex bounds for the maximum EM speed, power and torque. Similarly to the CVT model, we capture the EM efficiency with

$$P_{\text{ac}}(s) - P_{\text{m}}(s) = x_{\text{m}}(s)^{\top} Q_{\text{m}} x_{\text{m}}(s),$$

where $Q_{\text{m}} \in \mathbb{S}_{+}^{4}$ is a positive semi-definite matrix, and $x_{\text{m}}(s)$ is a vector containing the relevant in- and outputs, defined as

$$x_{\text{m}}(s) = \begin{bmatrix} \frac{1}{\sqrt{\omega_{\text{m}}(s)}} & \sqrt{\omega_{\text{m}}(s)} & \frac{P_{\text{m}}(s)}{\sqrt{\omega_{\text{m}}(s)}} & \frac{P_{\text{ac}}(s)}{\sqrt{\omega_{\text{m}}(s)}} \end{bmatrix}^{\top},$$

where $P_{\text{ac}}(s)$ represents the electrical EM power.

Since our framework optimizes the transmission design so that the EM is used as efficiently as possible, we strive to accurately capture the qualitative properties of the EM efficiency map. To this end, we additionally capture the optimal operating line of the EM, which we define as

$$\left. \frac{\partial \eta_{\text{m}}(T_{\text{m}}, \omega_{\text{m}})}{\partial \omega_{\text{m}}} \right|_{T_{\text{m}}, \omega_{\text{m}}^{*}(T_{\text{m}})} = 0,$$
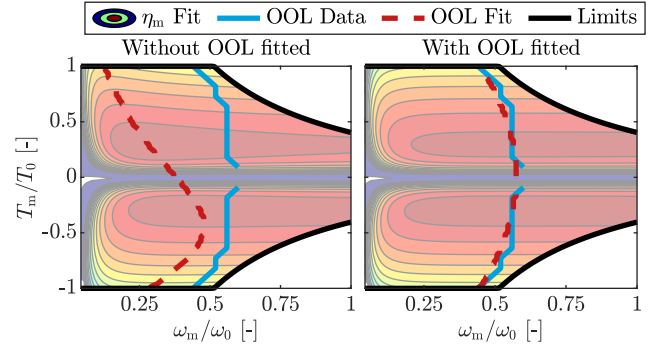

Fig. 4. EM maps showing the effect of fitting the optimal operating line (OOL). The figure on the left is obtained by optimizing the EM loss model without considering the optimal operating line, while the right figure is obtained by including the $x_{\text{m,o}}^{\top} Q_{\text{m}} e_1$ term in the semi-definite program.

where $\omega_{\text{m}}^{*}(T_{\text{m}})$ represents the optimal operating line, η_{m} is the EM efficiency and T_{m} is the EM torque. By differentiating our efficiency model with respect to the EM speed, as worked out in Appendix B, we can define the optimal operating line as

$$x_{\text{m,o}}^{\top} Q_{\text{m}} e_1 = 0,$$

with $e_1 = \begin{bmatrix} 1 & 0 & 0 & 0 \end{bmatrix}^{\top}$ and $x_{\text{m,o}} = x_{\text{m}}|_{T_{\text{m}}, \omega_{\text{m}}^{*}(T_{\text{m}})}$. Finally, we determine the fitting coefficients of the Q_{m} matrix by jointly fitting the losses and the optimal operating line, as

$$Q_{\text{m}} = \arg \min_{Q_{\text{m}} \in \mathbb{S}_{+}^{4}} \| P_{\text{ac}}(s) - P_{\text{m}}(s) - x_{\text{m}}(s)^{\top} Q_{\text{m}} x_{\text{m}}(s) \|_2$$
$$+ \| x_{\text{m,o}}^{\top} Q_{\text{m}} e_1 \|_2.$$

We normalize the power and speed data to keep the weight of the losses and optimal operating line equivalent, and solve the problem using semi-definite programming. The resulting loss model is shown in Fig. 3, whereas Fig. 4 shows the effect of including the optimal operating line in the model. By converting the power-based model to forces, we obtain the convex model

$$(F_{\text{ac}}(s) - F_{\text{m}}(s)) \cdot \frac{\gamma(s)}{r_{\text{w}}} \geq y_{\text{m}}(s)^{\top} Q_{\text{m}} y_{\text{m}}(s), \qquad (27)$$

with

$$y_{\mathrm{m}}(s) = \begin{bmatrix} \frac{\mathrm{d}t}{\mathrm{d}s}(s) & \frac{\gamma(s)}{r_{\mathrm{w}}} & F_{\mathrm{m}}(s) & F_{\mathrm{ac}}(s) \end{bmatrix}^{\top}, \quad (28)$$

where $F_{\mathrm{ac}}(s)$ is the electrical EM force.

We consider the limits of the EM in the force domain, similar to [22]. The maximum EM torque $T_{\mathrm{m,max}}$ constrains the mechanical EM force through

$$F_{\mathrm{m}}(s) \in [-1, 1] \cdot \frac{T_{\mathrm{m,max}} \cdot \gamma(s)}{r_{\mathrm{w}}}, \quad (29)$$

while the EM power limit is established with

$$F_{\mathrm{m}}(s) \in [-1, 1] \cdot \left(c_{\mathrm{m},1} \cdot \frac{\gamma(s)}{r_{\mathrm{w}}} + c_{\mathrm{m},2} \cdot \frac{\mathrm{d}t}{\mathrm{d}s}(s) \right), \quad (30)$$

with fitting coefficients $c_{\mathrm{m},1}$ and $c_{\mathrm{m},2}$. Finally, the maximum EM speed $\omega_{\mathrm{m,max}}$ is constrained with

$$\gamma(s) \le r_{\mathrm{w}} \cdot \frac{\mathrm{d}t}{\mathrm{d}s}(s) \cdot \omega_{\mathrm{m,max}}. \quad (31)$$

To vary the EM size, we scale the EM losses and limits linearly with respect to torque, similarly to [22]. We use scaling factor s_{m}, which is defined as

$$s_{\mathrm{m}} = \frac{T_{\mathrm{m,max}}}{T_{\mathrm{m0,max}}},$$

where $T_{\mathrm{m0,max}}$ represents the unscaled maximum EM torque. The maximum EM power is scaled similarly, as

$$c_{\mathrm{m},i} = c_{\mathrm{m0},i} \cdot s_{\mathrm{m}} \quad \forall i \in \{1, 2\},$$

where $c_{\mathrm{m0},i}$ represents an unscaled fitting coefficient.

E. Inverter

The inverter transforms the direct current from the battery into alternating current for the EM. We model the inverter losses similar to [29], using the quadratic model,

$$(F_{\mathrm{dc}}(s) - F_{\mathrm{ac}}(s)) \cdot \frac{\mathrm{d}t}{\mathrm{d}s}(s) \ge \alpha_{\mathrm{inv}} \cdot F_{\mathrm{ac}}^2(s), \quad (32)$$

where $F_{\mathrm{dc}}(s)$ is the force equivalent to the direct current inverter power, and α_{inv} is a quadratic fitting coefficient.

F. Battery

In this section we provide a quadratic battery loss model. We model the battery output force $F_{\mathrm{b}}(s)$ with

$$F_{\mathrm{b}}(s) = F_{\mathrm{dc}}(s) + P_{\mathrm{aux}} \cdot \frac{\mathrm{d}t}{\mathrm{d}s}(s), \quad (33)$$

where P_{aux} represents the power required for all auxiliary components in the vehicle, like electronics and cooling pumps. The battery losses are captured with

$$(F_{\mathrm{i}}(s) - F_{\mathrm{b}}(s)) \cdot \frac{\mathrm{d}t}{\mathrm{d}s}(s) \cdot P_{\mathrm{sc}} \ge F_{\mathrm{i}}^2(s), \quad (34)$$

where P_{sc} is the short-circuit power, which we assume to be constant.

G. Minimum-Lap-Time Optimization Problem

In this section, we distinguish between the different types of optimization variables, and solve the minimum-lap-time design and control problem in space-domain. From here on, we will drop the position dependence (s) in our notation when it is clear from context. First, we consider the design variables, $p = \gamma_1$ for the FGT, $p = \{\gamma_1, \ldots, \gamma_{n_{\mathrm{gear}}}\}$ for the MGT and $p = \gamma_{\mathrm{max}}$ for the CVT. For notational convenience, we model the design variables as state variables with zero dynamics,

$$\frac{\mathrm{d}\gamma_i(s)}{\mathrm{d}s} = 0, \quad (35)$$

which leaves only the initial conditions as free optimization variables. With this, we consider the state variables as $x = \{E_{\mathrm{bat}}, E_{\mathrm{kin}}, p\}$. We define the control inputs as $u = \{F_{\mathrm{m}}, F_{\mathrm{brk,F}}, F_{\mathrm{brk,R}}\}$, with the additional control input $\gamma(s)$ for the CVT and $b(s)$ for the MGT. Lastly, we define the remaining variables as lifting variables $z = \{v, \frac{\mathrm{d}t}{\mathrm{d}s}, F_{\mathrm{gb}}, F_{\mathrm{ac}}, F_{\mathrm{dc}}, F_{\mathrm{b}}, F_{\mathrm{i}}, F_{\mathrm{x,F}}, F_{\mathrm{x,R}}, F_{\mathrm{y,F}}, F_{\mathrm{y,R}}, F_{\mathrm{z,F}}, F_{\mathrm{z,R}}, F_{\mathrm{drag}}, F_{\mathrm{down}}\}$, and formulate the optimization problem as follows:

Problem 1 (Minimum-lap-time problem). *The time-optimal design and control strategies are the solution of*

$$\min_{x,u,z} \quad \int_0^S \frac{\mathrm{d}t}{\mathrm{d}s}(s)\mathrm{d}s,$$

$$\text{s.t.} \quad (1) - (19), (27) - (35),$$

$$\text{and} \quad \begin{cases} (20), (21) & \text{if FGT}, \\ (20), (22) & \text{if MGT}, \\ (23) - (26) & \text{if CVT}. \end{cases}$$

For both the FGT and CVT, Problem 1 is fully convex and can be solved for the globally optimal solution in polynomial time [30] using commercially available solvers. However, due to the discrete set $\mathbb{B}$ in constraint (22), the problem for the MGT is a non-convex MIOCP, which makes it computationally demanding to solve numerically.

III. MGT OPTIMIZATION METHODOLOGY

In this section, we propose an iterative algorithm to solve the MIOCP for the optimal design and control of an MGT-equipped race car. The algorithm is loosely based on Benders decomposition, as shown in Appendix E. First, we subdivide the MIOCP into a continuous optimization problem (COP), which optimizes the continuous design and control variables for a given gearshift trajectory, and a gearshift optimization problem (GOP), which optimizes the gearshifts for a given state and co-state trajectory. Then we provide the iterative algorithm itself, after which we conclude with a discussion regarding optimality and convergence criteria.

To distinguish between iterations of our algorithm, we introduce the $(\cdot)^k$ notation to describe the current iteration $k \in \mathbb{N}$. To improve readability, we separate the continuous inputs from the discrete input using $c = u \backslash b = \{F_{\mathrm{m}}, F_{\mathrm{brk,F}}, F_{\mathrm{brk,R}}\}$. Last, since the continuous inputs and lifting variables are optimized by both the COP and GOP, we distinguish between the results of the respective problems with a $(\cdot)_{\mathrm{C}}$ and $(\cdot)_{\mathrm{G}}$ notation.

A. Continuous Optimization Problem Definition

Since (22) contains a multiplication between the two optimization variables γ_i and b_i, it is not convex. We resolve this issue by removing $\gamma(s)$ from the optimization entirely by employing a Big-M formulation [31], which transforms a constraint of the form $f(\gamma(s)) \leq 0$, like (31), into the form

$$f(\gamma_i) \leq M \cdot (1 - b_i(s)) \ \forall i \in \{1, \ldots, n_{\text{gear}}\},$$

with M a scalar, significantly larger than $f(\gamma_i)$. By applying this transformation to constraints (27)-(31), as shown in Appendix C, we can define the optimization problem without $\gamma(s)$. The resulting problem is convex, except for the binary gearshift variable $b(s)$. However, by providing a pre-determined trajectory $b^{k-1}(s)$, we can define the convex COP:

Problem 2 (Continuous Optimization Problem). *We define the COP for MGT optimization as*

$$(x^k, c_{\text{C}}^k, z_{\text{C}}^k) = \arg\min_{x,c,z} \int_0^S \frac{\mathrm{d}t}{\mathrm{d}s}(s)\mathrm{d}s,$$

s.t.: State dynamics and limits: $(1) - (4), (35),$

            Vehicle dynamics: $(5) - (19),$

            Loss models: $(20), (32) - (34),$

            Big-M EM models: $(39) - (43),$

            $b(s) := b^{k-1}(s)$ $\forall s \in [0, S].$

This fully convex COP can be solved in polynomial time, similar to Problem 1 for the FGT and CVT.

B. Gearshift Optimization Problem Definition

We optimize the binary gearshift trajectory by applying PMP, which allows us to efficiently solve the problem for each position on track s independently. According to PMP [32], the optimal solution satisfies

$$(u^\star, z^\star) = \arg\min_{u,z} \mathcal{H}(x^\star, \lambda^\star, u, z), \tag{36}$$

where $(\cdot)^\star$ denotes an optimal trajectory, and $\mathcal{H}$ is the Hamiltonian, derived similar to [33] as

$$\mathcal{H}(s) = \frac{\mathrm{d}t}{\mathrm{d}s}(s) + \sum_{i=1}^{n_{\text{gear}}} (\lambda_{\gamma_i} \cdot 0) + \lambda_{\text{bat}}(s) \cdot (-F_{\text{i}}(s))$$
$$+ \lambda_{\text{kin}}(s) \cdot (F_{\text{x,F}}(s) + F_{\text{x,R}}(s) - F_{\text{drag}}(s) - F_{\text{g}}(s)),$$

where $\lambda_{\text{bat}}(s)$, $\lambda_{\text{kin}}(s)$, and $\lambda_{\gamma_i}(s)$ are the costates associated to the state integrators (1), (3) and (35), respectively. If we provide a pre-determined state and costate trajectory (x, λ), the Hamiltonian minimization problem can be solved at every position s independently, thereby significantly reducing the computational complexity. By minimizing the Hamiltonian for each gear option separately with convex optimization, the optimal trajectory can be determined by selecting the Hamiltonian with the minimum value at each position s. This yields n_{gear} convex optimization problems that can be solved in polynomial time. By providing a pre-determined state and costate trajectory $(x^k(s), \lambda^k(s))$, we can formulate the GOP as follows:

Problem 3 (Gearshift Optimization Problem). *We define the GOP for MGT optimization as*

$$(b^k, c_{\text{G}}^k, z_{\text{G}}^k) = \arg\min_{b,c,z} \mathcal{H}(s),$$

s.t.: Vehicle dynamics: $(5) - (19),$

            Loss models: $(20), (32) - (34),$

            Big-M EM models: $(39) - (43),$

$$\begin{cases} x(s) := x^k(s) \\ \lambda(s) := \lambda^k(s) \end{cases} \quad \forall s \in [0, S].$$

Note that the GOP uses a pre-determined (x^k, λ^k) trajectory, while omitting the state dynamics (1) and (3). Therefore its solution is not guaranteed to be feasible for Problem 1 without additional conditions, which we will provide in Section III-D.

C. Iterative Algorithm

This part of the thesis is dedicated to the proposal of an algorithm that optimizes the combined design and control of an MGT-equipped race car, by iterating between the COP and GOP until the trajectories converge. The criteria for convergence will be provided in Section III-D after discussing the feasibility and optimality of the problems. The iterative algorithm is described in Algorithm 1, and schematically shown in Fig. 5. Since iterating between the COP and GOP can result in a situation where the GOP jumps back and forth between two gearshift trajectories, we dampen the costate trajectories similar to [25], as

$$\tilde{\lambda}^k = \lambda^{k-1} + q \cdot \left(\lambda^k - \lambda^{k-1}\right),$$

where $\tilde{\lambda}^k$ is the damped trajectory and $q \in [0, 1]$ is the damping coefficient. At convergence, when $\lambda^k = \lambda^{k-1}$, the damping becomes irrelevant and yields $\tilde{\lambda}^k = \lambda^k$.

Algorithm 1: Iterative algorithm for the optimization of an electric race car equipped with an MGT.

$k \leftarrow 1, \ b^0 \leftarrow$ Derive initial strategy;

while *not converged* **do**

     $(x^k, \lambda^k, c_{\text{C}}^k, z_{\text{C}}^k) \leftarrow$ Solve COP(b^{k-1});

     if $k > 1$ **then**

         $\tilde{\lambda}^k \leftarrow \lambda^{k-1} + q \cdot \left(\lambda^k - \lambda^{k-1}\right)$;

     else

         $\tilde{\lambda}^k \leftarrow \lambda^k$

     end

     $(b^k, c_{\text{G}}^k, z_{\text{G}}^k) \leftarrow$ Solve GOP$(x^k, \tilde{\lambda}^k)$;

     if *satisfied* (37) *and* (38) **then**

         $(x^\star, b^\star, c^\star, z^\star) \leftarrow (x^k, b^k, c_{\text{C}}^k, z_{\text{C}}^k)$;

         Stop;

     end

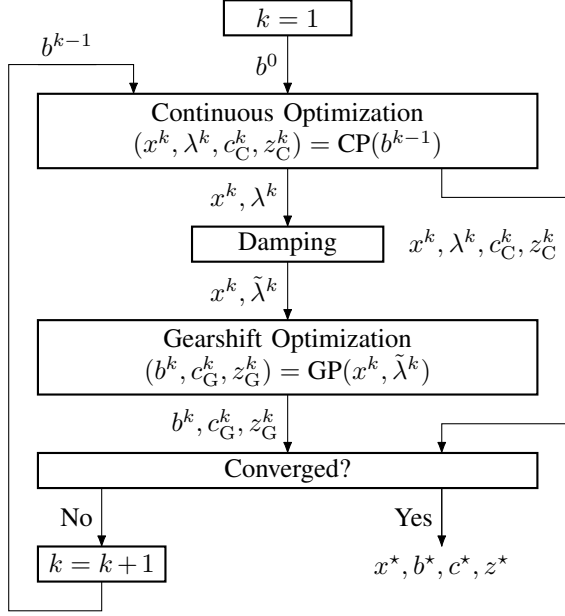 $k \leftarrow k + 1$;

end

Fig. 5. Iterative algorithm for the optimization of an electric race car equipped with an MGT.

D. Discussion of Optimality and Convergence

In order to devise convergence criteria for the iterative algorithm, this section establishes conditions for the feasibility and optimality of the COP and the GOP.

Lemma 1. *If the COP yields a feasible solution, this solution is also feasible for Problem 1.*

Proof. Since the feasible domain of the COP is a subset of the feasible domain of Problem 1, any solution that is feasible for the COP is inherently also feasible for Problem 1. □

Lemma 2. *Consider the case where the GOP gear trajectory is equal for two iterations, $b^k = b^{k-1}$, and where $\tilde{\lambda}^k = \lambda^k$. If the c_C^k, z_C^k trajectory resulting from the COP is feasible and equal to the c_G^k, z_G^k trajectory resulting from the GOP, then the GOP solution is feasible for Problem 1.*

Proof. Suppose, for contradiction, that there exists a GOP solution $(x^k, \tilde{\lambda}^k, b^k, z_G^k, c_G^k)$ that is infeasible for Problem 1, while it is equal to the COP solution $(x^k, \lambda^k, b^{k-1}, z_C^k, c_C^k)$. This implies that the COP solution is also infeasible for Problem 1, since the solutions are equal. However, Lemma 1 states that any feasible COP solution is also feasible for Problem 1, which is a contradiction. □

Lemma 3. *If the trajectory b^{k-1}, which is fed into the COP, is globally optimal for Problem 1, then the resulting trajectory $(x^k, \lambda^k, c_C^k, z_C^k)$ is also globally optimal for Problem 1.*

Proof. Since the COP is convex, its solution is globally optimal for the given b^{k-1} trajectory [30]. Therefore, if the b^{k-1} trajectory is globally optimal for Problem 1, the $(x^k, \lambda^k, c_C^k, z_C^k)$ solution to the COP is also globally optimal for Problem 1. □

Lemma 4. *Consider the case where the GOP is fed with the (x^k, λ^k) trajectory that is globally optimal for Problem 1. If the GOP solution, (b^k, c_G^k, z_G^k), is unique, as well as feasible for Problem 1, then it is also globally optimal for Problem 1.*

Proof. First, consider that the GOP and Problem 1 have equivalent constraints, except that the GOP constrains the (x, λ) trajectory, while not containing constraints (1)-(4). Therefore, the feasible domain of Problem 1 is a subset of the feasible domain of the GOP for the fixed globally optimal $(x^\star, \lambda^\star)$. Second, consider that according to (36), the GOP solution (b^k, c_G^k, z_G^k) is globally optimal for the provided (x^k, λ^k) trajectory, if it is unique. Therefore, if the GOP solution is unique, but not globally optimal for Problem 1, then it is either not feasible for Problem 1, or the (x^k, λ^k) trajectory fed into the GOP is not globally optimal for Problem 1. □

In order to obtain a potential candidate for optimality, the solution of the iterative algorithm should satisfy the feasibility and optimality conditions from Lemma 1-4, which we implement as

$$\|(y^k - y^{k-1})\|_\infty \leq \epsilon \quad \forall y \in \{b, x, \lambda\}, \tag{37}$$

$$\|(y_G^k - y_C^k)\|_\infty \leq \epsilon \quad \forall y \in \{c, z\}, \tag{38}$$

where ϵ is a small normalized scalar to allow for numerical tolerances. If these conditions are satisfied, the algorithm is terminated.

Since the COP and GOP both minimize the lap time, iterating between the two will improve the lap time to a point where neither problem can independently improve the lap time further. At this point, the gear trajectory will remain the same for multiple iterations, and (37) will be satisfied. When considering a fixed (b, x, λ) trajectory, both the COP and GOP will consider the same (c, z) trajectory to be optimal. Therefore, at convergence, (38) will be satisfied as well. In conclusion, the algorithm will converge to a situation where the convergence criteria are satisfied, and where the GOP solution is feasible for Problem 1.

Lastly, if either the COP or the GOP finds the globally optimal trajectory, Lemmas 3 and 4 state that the algorithm will converge at this point if the GOP solution is unique. This gives us some confidence in the quality of our results, and even though we can only provide necessary conditions for optimality, our numerical results provided in Section IV do indicate that our algorithm provides a promising candidate for the optimal solution.

IV. RESULTS AND VALIDATION

This section presents the numerical results obtained by applying our framework to various transmission types. First, we evaluate the performance of a race car equipped with an FGT, a CVT, a 2-speed MGT (2GT), a 3-speed MGT (3GT) and a 4-speed MGT (4GT). Second, we compare the performance for multiple battery energy limits and EM sizes, and lastly, we verify the accuracy of our EM and CVT models, and validate the performance of our iterative algorithm.
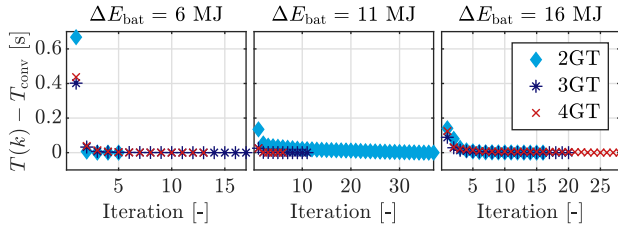
Fig. 6. Convergence of the iterative algorithm, showing the difference between the lap time at each iteration and the final converged lap time (T_{conv}).
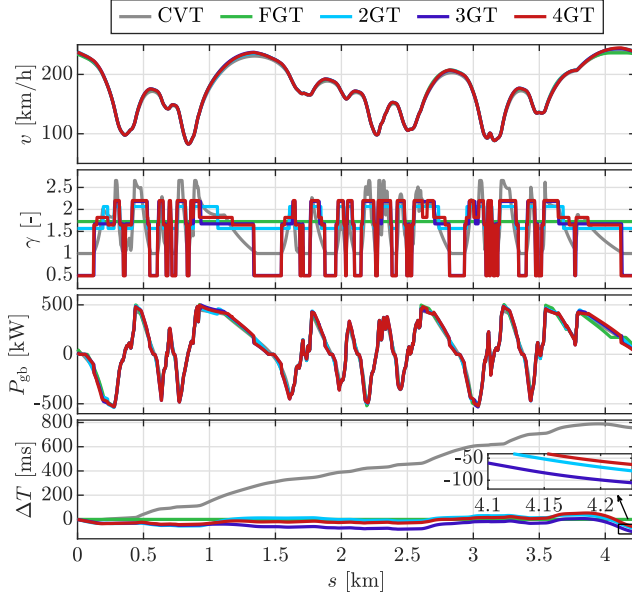

Fig. 7. Velocity, gear ratio, and transmission output power trajectories for each car, with $\Delta E_{\text{bat}} = 11\,\text{MJ}$. To compare, we also show the relative lap time of each car with respect to the FGT-equipped car.

A. Numerical Results

In this section, we apply our framework to one lap around the 4.2 km long Zandvoort race track, using the InMotion LMP3 race car [34] as a demonstrator. We solve Problem 1 for the FGT- and CVT-equipped cars, and apply the iterative algorithm for the cars with a 2GT, a 3GT and a 4GT. The parameters which distinguish the transmission types can be found in Table II of Appendix D. We parse the cone programs with YALMIP [35], using a forward Euler discretization of $\Delta s = 4\,\text{m}$, and solve with MOSEK [36] on a laptop with a 2.6 GHz processor and 16 GB RAM. Problem 1 takes on average 1.2 s to solve for the FGT and 1.4 s for the CVT, while the iterative algoritm takes on average 63 s to converge. A detailed breakdown of the computation times for each problem is shown in Table III of Appendix D. As initial guess for the gearshift, we use a strategy where the full lap is driven in first gear, except for one discrete step in each other gear. This way, solving the COP yields multiple distinct gear ratios, which allows the GOP to derive an improved gearshift strategy.

In Fig. 6, we show the convergence behavior of the iterative algorithm. As can be observed, the algorithm gets close to
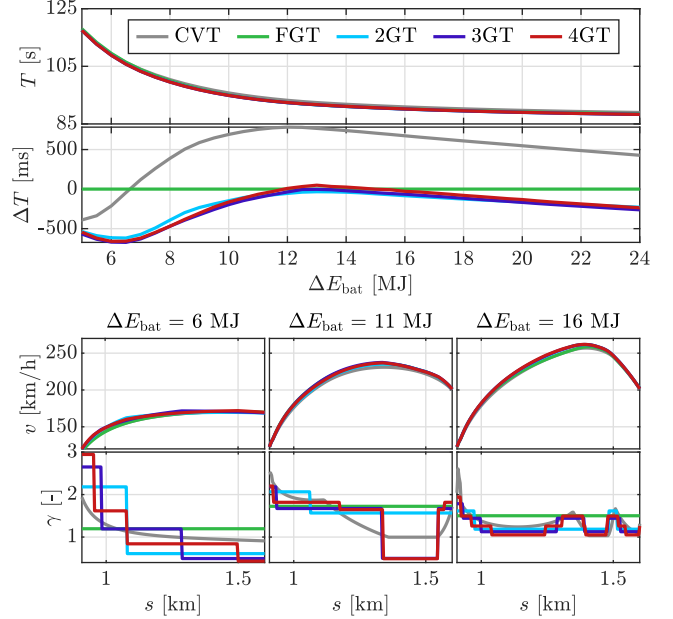

Fig. 8. Comparison between the lap times obtained by race cars equipped with different transmission types. The results are shown over a range of battery energy limits, specifically showing the relative lap times with respect to the FGT-equipped car. We further show the velocity and gear ratio trajectories for 3 battery energy limits to clarify the difference in lap times.

the final converged lap time within a few iterations, while there is no definitive correlation between the number of gears and the amount of iterations required for convergence. In Fig. 7, we present the results for a battery energy limit of $\Delta E_{\text{bat}} = 11\,\text{MJ}$, for which the vehicle is significantly energy-limited. As can be observed, the CVT-equipped car performs considerably worse than the other cars. Even though the CVT improves the EM efficiency with 1.2 % compared to the FGT, its own average efficiency is 1 % lower than that of the FGT. In combination with its increased weight, this still causes an increase in lap time. The 2GT-car, on the other hand, outperforms the FGT-car by having an increased EM efficiency and by being able to accelerate faster and regeneratively brake both later and more aggressively. The 3GT-car contains an added gear with a very low ratio, which allows for a high EM efficiency at high speed but low power sections. In combination with a higher first gear ratio, this allows the 3GT-car to accelerate faster out of corners compared to the 2GT-car, yielding even faster lap times. The 4GT-car, however, cannot provide enough additional performance with its added gear to make up for its higher weight, making it marginally slower than the 2GT-car.

To understand the effect of the available battery energy on the optimal transmission type, Fig. 8 shows the performance over a range of battery energy limits, together with the acceleration behavior at a representative straight track section for three battery energy limits. As can be observed, compared to the FGT- and CVT-cars, all three MGT-cars show similar
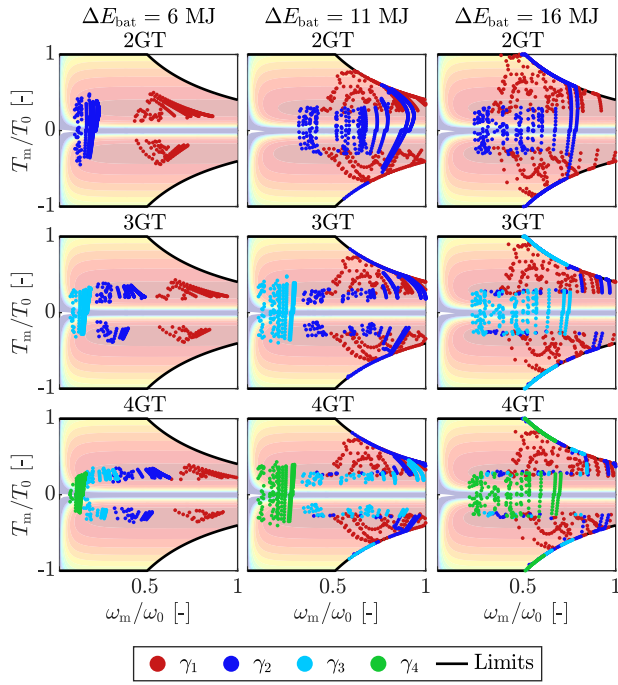
Fig. 9. Operating points of the EM for each MGT-equipped car. We specifically show the operating points for 3 battery energy limits to showcase the different utilization of each gear in each scenario.
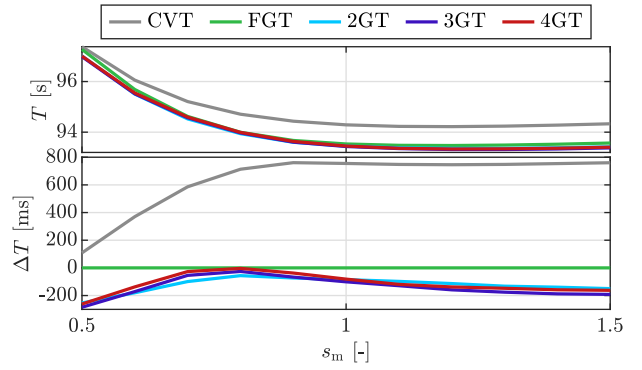

Fig. 10. Comparison between the lap times obtained by race cars equipped with different transmission types over a range of EM sizes for $\Delta E_{\text{bat}} = 11$ MJ. We specifically show the relative lap times with respect to the FGT-equipped car.
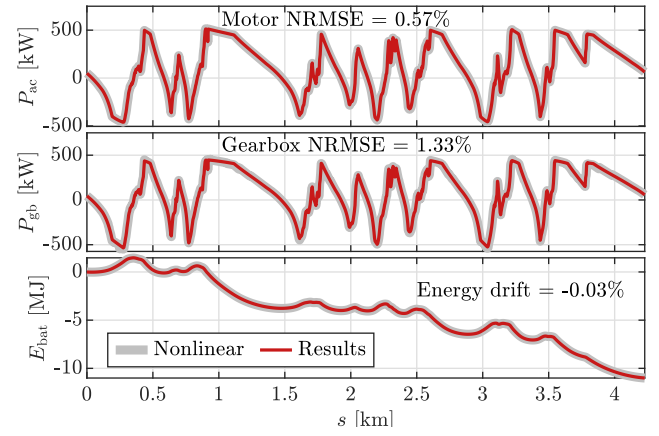

Fig. 11. Comparison between the convex and nonlinear EM and CVT models, and the resulting battery energy drift for $\Delta E_{\text{bat}} = 11$ MJ.

behavior, having better lap times for low energy levels due to increased powertrain efficiency, while also performing better at high energy levels due to superior acceleration performance. However, around $\Delta E_{\text{bat}} = 13$ MJ, neither the increased efficiency nor the acceleration performance have enough effect to overcome the additional component weight, making only the 2GT-car marginally faster than the FGT-car. In Fig. 9, the operating points of the EM can be seen for all three MGT-cars and for multiple battery energy limits. Observe that for $\Delta E_{\text{bat}} = 6$ MJ, each additional gear is used to get the EM operation closer to its peak efficiency, while for $\Delta E_{\text{bat}} = 16$ MJ, each additional gear is used to increase the time spent at maximum power.

To better understand the role the transmission can play in optimizing the size of the EM, Fig. 10 shows the lap time for a range of EM sizes. Note that a similar pattern can be seen for the EM size as for the battery energy limit, while the underlying reason is the opposite. For small EM sizes, the MGT-cars can better exploit the maximum power area of the EM, while for large EM sizes, the MGTs improve the EM efficiency, making more energy available for acceleration. Overall, the EM size at which the fastest lap time is obtained is virtually the same for each car, due to the strong influence of the EM size on the vehicle weight.

In conclusion, all three MGT-equipped cars generally outperform the FGT- and CVT-cars. Based on the situation, either the 2GT-car or 3GT-car delivers the best performance, while the 4GT-car is not able to make its 4th gear worth its weight in lap time gain.

B. Validation

In this section, we first validate the accuracy of the EM and CVT models, after which we evaluate the quality of the iterative algorithm by solving part of the lap using a state-of-the-art mixed-integer optimizer. Last, we verify that the lap time of an idealized MGT-car with increasingly more gears converges to that of an idealized CVT-car.

In Fig. 11, we compare the performance of the convex model with that of a nonlinear model that directly employs the efficiency maps of the EM and CVT. By recomputing the energy consumption based on the losses of the nonlinear model, we can observe that the total drift in energy consumption reaches only 0.03 % for $\Delta E_{\text{bat}} = 11$ MJ. Over the full range of battery energy limits, the average drift reaches 1.31 %, while the maximum drift reaches 1.78 %.

In order to validate the efficacy of the iterative algorithm, we solve the MIOCP directly using the MOSEK mixed-integer second-order cone programming solver, which employs a branch-and-bound algorithm to solve the problem with global optimality guarantees. However, due to the complex nature

	Mixed-integer		Iterative		
N_{steps}	Solving time	Section time	Solving time	Section time	Section time difference
12	43 s	3.5946 s	2 s	3.5946 s	0.0 ms
14	120 s	3.4959 s	2 s	3.4959 s	0.0 ms
16	575 s	3.4256 s	2 s	3.4259 s	0.3 ms
18	1940 s	3.3403 s	2 s	3.3403 s	0.0 ms
20	8153 s	3.4759 s	2 s	3.4759 s	0.0 ms
22	34915 s	3.4302 s	2 s	3.4302 s	0.0 ms

Fig. 12. Comparison between the lap times of an ideal CVT (iCVT) and an ideal MGT (iMGT) for $\Delta E_{\text{bat}} = 11\,\text{MJ}$. Additionally, we show the gear ratio trajectories of the iCVT and an ideal 22-speed MGT (i22GT).

of our problem, the mixed-integer solver can only solve for a discretization of $N_{\text{steps}} = 22$ steps in less than 10 hours. Since the original problem contains $N_{\text{steps}} = 1058$ steps, this means that the mixed-integer solver can only solve only around 2 % of the lap within 10 hours. Therefore, we validate the iterative algorithm by using a coarser discretization, and by optimizing only a small section of the track, containing a braking zone, a corner, and an acceleration zone. Since Lemma 3 states that the COP will return the globally optimal solution if it is fed with the globally optimal binary gearshift trajectory, we expect equal results if the mixed-integer solver finds the same gearshift trajectory. To exemplify the computational complexity of our problem, we present the computation times for the mixed-integer algorithm and iterative algorithm for a varying number of discretization steps in Table I. As can be observed, the mixed-integer algorithm soon becomes intractable, while the iterative algorithm obtains virtually the same section times in much less computation time. For only one simulation is the section time obtained by the iterative algorithm 0.3 milliseconds slower, due to a poor initial guess. This confirms that the iterative algorithm provides us with a promising candidate for optimality.

Lastly, to verify the performance and robustness of the iterative algorithm on the entire lap, we compare the performance of an idealized MGT- and CVT-equipped car, ignoring the transmission weights, efficiencies and ratio limits. Since a CVT is essentially an MGT with an infinite number of gears, simulating the MGT-car with an increasing number of gears should result in a lap time approximating that of the CVT-car. As can be seen in Fig. 12, the results neatly converge to a difference in lap time below 10 ms at 22 speeds, showing that our algorithm functions for large numbers of gears.

V. CONCLUSION

In this thesis, we presented an efficient algorithm to optimize the design and control of an electric race car, considering a continuously variable transmission (CVT), a fixed-gear transmission (FGT) and a multiple-gear transmission (MGT). We derived convex models for the system components, and developed an iterative algorithm to efficiently handle the mixed-integer nature of the MGT gearshifts, by combining convex optimization and Pontryagin's Minimum Principle (PMP). We provided necessary conditions for the optimality of our solution, and showed that our algorithm can converge
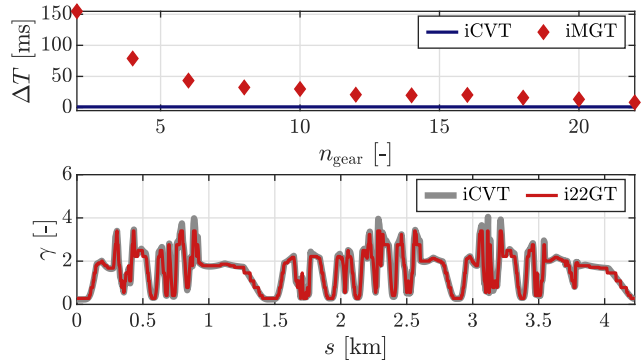
to the globally optimal solution, whilst our results showed that our algorithm indeed provides a promising candidate for the optimal solution. Furthermore, we studied the performance of the various transmission types on the Zandvoort race track for multiple battery energy limits and EM sizes. We observed that an MGT can balance the respective advantages of an FGT and a CVT, by delivering significant control over the EM operating range at a low cost. However, we also noted that adding too many gears can be detrimental to the lap time, highlighting that careful optimization is required.

The efficiency of our framework opens the door for future research to investigate the optimal transmission design when considering a full race season. When optimizing over a number of race tracks, we expect that the performance of the CVT- and 4GT-equipped cars will improve due to their control flexibility. Furthermore, steps could be taken to improve the accuracy of the modeling components, for example by considering thermal EM limitations, gearshift losses, or more accurate weight and efficiency models for the individual MGT components.

APPENDIX A
SECOND-ORDER CONE PROGRAM

All quadratic models used in our optimization problems are of the form

$$y_1 \cdot y_2 \geq y_3^2, \quad \text{with } y_3^2 \geq 0,$$

which we can reformulate as the second-order cone constraint (SOCC)

$$y_1 + y_2 \geq \left\| \begin{matrix} 2 \cdot y_3 \\ y_1 - y_2 \end{matrix} \right\|_2 .$$

For the kinetic energy and lethargy equations, (5) and (6), as well as for the inverter and battery loss models, (32) and (34), this implementation is trivial. However, for the CVT and EM models, (25) and (27), an intermediate step is required. By using a Cholesky factorization,

$$x^\top Q x = x^\top C^\top C x, \quad \text{with } Q \in \mathbb{S}^+,$$

we can now formulate the models as SOCCs with $y_3 = Cx$.

APPENDIX B
MOTOR MODEL

In this appendix we work out how to incorporate the optimal operating line into the EM loss model. We consider

$$\left. \frac{\partial \eta_m(T_m, \omega_m)}{\partial \omega_m} \right|_{T_m, \omega_m^*(T_m)} = 0,$$

with the EM efficiency η_m, defined as

$$\eta_m = \left(\frac{P_m}{P_m + x_m^\top Q_m x_m} \right)^{\text{sign}(P_m)},$$

with

$$P_m = T_m \cdot \omega_m.$$

We additionally define

$$z_m = \frac{x_m}{\sqrt{\omega_m}} = \begin{bmatrix} \frac{1}{\omega_m} & 1 & T_m & T_{ac} \end{bmatrix}^\top,$$

and

$$\frac{\partial \left(z_m^\top Q_m z_m \right)}{\partial \omega_m} = -\frac{2}{\omega_m^2} z_m^\top Q_m e_1.$$

By substitution, we obtain for $P_m > 0$

$$0 = \frac{\partial \left(\frac{T_m \omega_m}{T_m \omega_m + x_m^\top Q_m x_m} \cdot \left(\frac{\frac{1}{\omega_m}}{\frac{1}{\omega_m}} \right) \right)}{\partial \omega_m},$$

which we can differentiate with respect to ω_m, yielding

$$0 = \frac{0 + T_m \frac{2}{\omega_m^2} z_m^\top Q_m e_1}{\left(T_m + z_m^\top Q_m z_m \right)^2}.$$

By eliminating all scaling factors that do not influence the coefficients of the Q_m matrix, we finally obtain the result,

$$0 = x_m^\top Q_m e_1.$$

Using the same methodology for $P_m < 0$ yields the same result, providing us a way to incorporate the optimal operating line into the EM loss model.

APPENDIX C
BIG-M FORMULATION

We define the Big-M EM loss model as

$$(F_{ac}(s) - F_m(s)) \cdot \frac{\gamma_i}{r_w} \geq y_{m,\gamma}^\top(s) Q_m y_{m,\gamma}(s) \\ - M \cdot (1 - b_i(s)), \quad (39)$$

with

$$y_{m,\gamma}(s) = \begin{bmatrix} \dfrac{dt}{ds}(s) & \dfrac{\gamma_i}{r_w} & F_m(s) & F_{ac}(s) \end{bmatrix}^\top. \quad (40)$$

For the EM torque limit, we define

$$F_m(s) \in [-1, 1] \cdot \left(\frac{T_{m,max} \cdot \gamma_i}{r_w} + M \cdot (1 - b_i(s)) \right), \quad (41)$$

while for the EM power limit, we define

$$F_m(s) \in [-1, 1] \cdot \left(c_{m,1} \cdot \frac{\gamma_i}{r_w} \right. \\ \left. + c_{m,2} \cdot \frac{dt}{ds}(s) + M \cdot (1 - b_i(s)) \right), \quad (42)$$

and lastly, for the EM speed limit, we define

$$\gamma_i \leq r_w \cdot \frac{dt}{ds}(s) \cdot \omega_{m,max} + M \cdot (1 - b_i(s)). \quad (43)$$

APPENDIX D
VEHICLE PARAMETERS AND OPTIMIZATION RESULTS

The parameters that change between the various transmission types can be seen in Table II, while Table III shows the computation times for our framework. Note that mainly the GOP computation time is strongly influenced by the number of gears, since it has to solve a convex optimization problem for each possible gear option.

TABLE II
RELEVANT VEHICLE PARAMETERS

Parameter	Symbol	Value
Mass base vehicle	m_0	1315 kg
Mass CVT	m_{cvt}	70 kg
Mass geared transmission excluding gears	m_{gb0}	30 kg
Mass per gear	m_{gear}	5 kg
Mass unscaled EM	m_{m0}	58 kg
Efficiency FGT	η_{fgt}	97 %
Efficiency MGT	η_{mgt}	97 %

TABLE III
COMPUTATION TIMES, AVERAGED OVER 130 MEASUREMENTS

	COP	GOP	Iterations	Total runtime
CVT	-	-	1	1.36 s
FGT	-	-	1	1.17 s
2GT	1.54 s	1.39 s	10	29.28 s
3GT	1.87 s	2.03 s	16	60.84 s
4GT	2.20 s	2.69 s	20	98.26 s

The Benders decomposition is a technique that can be used to solve our MIOCP by decomposing the original problem into a sub-problem and master problem. The sub-problem yields a feasible solution and upper bound for the original problem using convex optimization on a known discrete trajectory, while the master problem yields a lower bound for the solution of the original problem using mixed-integer linear programming. By iterating between these problems, the upper and lower bound converge towards each other until a satisfactory optimality gap is obtained. In this appendix we describe how the Benders decomposition could be implemented for Problem 1. We first describe the sub-problem and master problem, after which we shortly discuss the iterative algorithm and the issues with applying it to our problem. For further information regarding the Benders decomposition we refer the reader to [37].

A. Sub-problem

The sub-problem for the Benders decomposition is very similar to our COP, using a big-M formulation and pre-determined gearshift trajectory b^k. Similarly to our algorithm we employ the $(\cdot)^k$ notation to describe the current iteration $k \in \mathbb{N}^+$. We formulate the Benders sub-problem as:

Problem 4 (Benders Sub-Problem). *We define the Benders sub-problem for MGT optimization as*

$$T_{\mathrm{UB}}^k = \min_{x,c,z} \int_0^S \frac{\mathrm{d}t}{\mathrm{d}s}(s)\mathrm{d}s,$$

$$
\begin{array}{lll}
\text{s.t.: State dynamics and limits:} & (1)-(4),(35), \\
\text{Vehicle dynamics:} & (5)-(19), \\
\text{Loss models:} & (20),(32)-(34), \\
\text{Big-M EM models:} & (39)-(43), \\
b(s) := b^k(s) \quad : \lambda_{\mathrm{b}}^k(s) & \forall s \in [0,S].
\end{array}
$$

This problem is solved using convex optimization, yielding T_{UB}^k, and the dual trajectory to $b(s) := b^k(s)$, defined as λ_{b}^k.

B. Master problem

In the Benders master problem, the gearshift trajectory b^k and a lower bound for the optimal solution T_{LB}^k are determined, by adding a so-called "cutting plane" in each iteration. We formulate the Benders master problem as follows:

Problem 5 (Benders Master Problem). *We define the Benders master problem for MGT optimization as*

$$T_{\mathrm{LB}}^k = \min_{\alpha, b^k} \alpha$$

$$
\begin{array}{l}
\text{s.t.: } \alpha \geq -M \\
\alpha \geq T_{\mathrm{UB}}^j + \lambda_{\mathrm{b}}^j \left(b^k - b^j\right) \quad \forall j \in \{1,\ldots,k-1\}
\end{array}
$$

with optimization variable $\alpha \in \mathbb{R}$ and with M a significantly large scalar which provides a lower bound to the problem in the first iteration.

This problem is solved using mixed-integer linear programming, yielding T_{LB}^k, b^k.

C. Iterative algorithm and discussion

The strategy for solving the Benders decomposition is shown in Algorithm 2.

Algorithm 2: Benders decomposition algorithm.

$i \leftarrow 1$, $T_{\mathrm{LB}}^1 \leftarrow -\infty$, $b^1 \leftarrow$ Derive initial strategy;
while *not converged* **do**
    $(T_{\mathrm{UB}}^k, \lambda_{\mathrm{b}}^k) \leftarrow$ Solve sub-problem;
    if $T_{\mathrm{UB}}^k - T_{\mathrm{LB}}^k \leq \epsilon$ **then**
        $T^\star \leftarrow T_{\mathrm{UB}}^j$;
        Stop;
    end
    $(T_{\mathrm{LB}}^k, b^k) \leftarrow$ Solve master problem;
    $k \leftarrow k+1$;
end

The issue with using the Benders decomposition for our problem is that a large number of cutting planes is required for the algorithm to converge. Since the master problem is still a mixed-integer optimization problem, it does not provide polynomial time convergence guarantees. While the problem can be solved efficiently for the first few iterations, the complexity increases as more cuts are required. Due to the particularities of our problem with a relatively long horizon, the Benders decomposition requires a large number of cuts, making it an inefficient method for solving our problem. Our GOP is inspired by the Benders master problem, but to make it more computationally efficient, we decompose the problem so that it can be solved for each position separately. This significantly decreases the computational complexity, while we no longer obtain a lower bound for our problem.

REFERENCES

[1] IEA, "Global EV outlook 2021," International Energy Agency, Tech. Rep., 2021.

[2] S. Sager, "Numerical methods for mixed–integer optimal control problems," Ph.D. dissertation, Universität Heidelberg, 01 2006.

[3] C. Lin, J. Kang, J. W. Grizzle, and H. Peng, "Energy management strategy for a parallel hybrid electric truck," in *American Control Conference*, 2001.

[4] J. Ritzmann, A. Christon, M. Salazar, and C. H. Onder, "Fuel-optimal power split and gear selection strategies for a hybrid electric vehicle," in *SAE Int. Conf. on Engines & Vehicles*, 2019.

[5] J. van den Hurk and M. Salazar, "Energy-optimal design and control of electric vehicles' transmissions," in *IEEE Vehicle Power and Propulsion Conference*, 2021, in press. Extended version available at https://arxiv.org/abs/2105.05119.

[6] N. Robuschi, M. Salazar, P. Duhr, F. Braghin, and C. H. Onder, "Minimum-fuel engine on/off control for the energy management of hybrid electric vehicles via iterative linear programming," in *Symposium on Advances in Automotive Control*, 2019.

[7] V. Ngo, T. Hofman, M. Steinbuch, and A. Serrarens, "Optimal control of the gearshift command for hybrid electric vehicles," *IEEE Transactions on Vehicular Technology*, vol. 61, no. 8, pp. 3531–3543, Oct 2012.

[8] T. Nüesch, P. Elbert, M. Flankl, C. H. Onder, and L. Guzzella, "Convex optimization for the energy management of hybrid electric vehicles considering engine start and gearshift costs," *Energies*, vol. 7, no. 2, pp. 834–856, 2014.

[9] N. Robuschi, M. Salazar, N. Viscera, F. Braghin, and C. H. Onder, "Minimum-fuel energy management of a hybrid electric vehicle via iterative linear programming," *IEEE Transactions on Vehicular Technology*, vol. 69, no. 12, pp. 14 575–14 587, 2020.

[10] N. Robuschi, C. Zeile, S. Sager, and F. Braghin, "Multiphase mixed-integer nonlinear optimal control of hybrid electric vehicles," *Automatica*, vol. 123, no. 109325, 2021. [Online]. Available: https://www.sciencedirect.com/science/article/pii/S0005109820305252

[11] M. Joševski and D. Abel, "Gear shifting and engine on/off optimal control in hybrid electric vehicles using partial outer convexification," in *2016 IEEE Conference on Control Applications (CCA)*, 2016, pp. 562–568.

[12] V. Saini, S. Singh, S. Nv, and H. Jain, "Genetic algorithm based gear shift optimization for electric vehicles," *SAE Int. Journal of Alternative Powertrains*, vol. 5, no. 2, pp. 348–356, 2016.

[13] A. Fofana, O. Haas, V. Ersanilli, K. Burnham, J. Mahtani, C. Woolley, and K. Vithanage, "Multi-objective genetic algorithm for an automatic transmission gear shift map," *IFAC-PapersOnLine*, vol. 49, no. 3, pp. 123–128, 2016.

[14] B. Gao, Q. Liang, Y. Xiang, L. Guo, and H. Chen, "Gear ratio optimization and shift control of 2-speed i-amt in electric vehicle," *Mechanical Systems and Signal Processing*, vol. 50-51, pp. 615–631, 2015.

[15] H. Yu, F. Zhang, J. Xi, and D. Cao, "Mixed-integer optimal design and energy management of hybrid electric vehicles with automated manual transmissions," *IEEE Transactions on Vehicular Technology*, vol. 69, no. 11, pp. 12 705–12 715, 2020.

[16] P. Leise, L. Altherr, N. Simon, and P. F. Pelz, "Finding global-optimal gearbox designs for battery electric vehicles," in *World Congress on Global Optimization*, 2019.

[17] S. Terwen, M. Back, and V. Krebs, "Predictive powertrain control for heavy duty trucks," *IFAC Proceedings Volumes*, vol. 37, no. 22, pp. 105–110, 2004, iFAC Symposium on Advances in Automotive Control 2004, Salerno, Italy, 19-23 April 2004. [Online]. Available: https://www.sciencedirect.com/science/article/pii/S1474667017303294

[18] T. Hofman and M. Salazar, "Transmission ratio design for electric vehicles via analytical modeling and optimization," in *IEEE Vehicle Power and Propulsion Conference*, 2020.

[19] F. J. R. Verbruggen, M. Salazar, M. Pavone, and T. Hofman, "Joint design and control of electric vehicle propulsion systems," in *European Control Conference*, 2020.

[20] M. Konda, T. Hofman, and M. Salazar, "Energy-optimal design and control of electric powertrains under motor thermal constraints," in *European Control Conference*, 2022, in press. Available online at https://arxiv.org/abs/2111.07711.

[21] S. Ebbesen, M. Salazar, P. Elbert, C. Bussi, and C. H. Onder, "Time-optimal control strategies for a hybrid electric race car," *IEEE Transactions on Control Systems Technology*, vol. 26, no. 1, pp. 233–247, 2018.

[22] O. Borsboom, C. A. Fahdzyana, T. Hofman, and M. Salazar, "A convex optimization framework for minimum lap time design and control of electric race cars," *IEEE Transactions on Vehicular Technology*, vol. 70, no. 9, pp. 8478–8489, 2021.

[23] A. Locatello, M. Konda, O. Borsboom, T. Hofman, and M. Salazar, "Time-optimal control of electric race cars under thermal constraints," in *European Control Conference*, 2021.

[24] S. Broere and M. Salazar, "Minimum-lap-time control strategies for all-wheel drive electric race cars via convex optimization," in *European Control Conference*, 2022, in press. Available online at https://arxiv.org/abs/2111.04650.

[25] P. Duhr, G. Christodoulou, C. Balerna, M. Salazar, A. Cerofolini, and C. H. Onder, "Time-optimal gearshift and energy management strategies for a hybrid electric race car," *Applied Energy*, vol. 282, no. 115980, 2020.

[26] C. Balerna, M.-P. Neumann, N. Robuschi, P. Duhr, A. Cerofolini, V. Ravaglioli, and C. Onder, "Time-optimal low-level control and gearshift strategies for the formula 1 hybrid electric powertrain," *Energies*, vol. 14, no. 1, 2021. [Online]. Available: https://www.mdpi.com/1996-1073/14/1/171

[27] J. van Kampen, T. Herrmann, T. Hofman, and M. Salazar, "Optimal endurance race strategies for a fully electric race car under thermal constraints," *IEEE Transactions on Control Systems Technology*, 2023, submitted.

[28] C. E. Douglas and A. Thite, "Effect of lubricant temperature and type on spur gear efficiency in racing engine gearbox across full engine load and speed range," *Proceedings of the Institution of Mechanical Engineers, Part J: Journal of Engineering Tribology*, vol. 229, no. 9, pp. 1095–1113, 2015. [Online]. Available: https://doi.org/10.1177/1350650115574305

[29] J. van Kampen, T. Herrmann, and M. Salazar, "Maximum-distance race strategies for a fully electric endurance race car," *European Journal of Control*, 2022, in press. Available online at https://arxiv.org/abs/2111.05784.

[30] S. Boyd and L. Vandenberghe, *Convex optimization*. Cambridge Univ. Press, 2004.

[31] A. Richards and J. How, "Mixed-integer programming for control," in *American Control Conference*, 2005.

[32] D. Bertsekas, *Dynamic programming and optimal control*, 4th ed. Athena Scientific, 1995.

[33] M. Salazar, P. Elbert, S. Ebbesen, C. Bussi, and C. H. Onder, "Time-optimal control policy for a hybrid electric race car," *IEEE Transactions on Control Systems Technology*, vol. 25, no. 6, pp. 1921–1934, 2017.

[34] "InMotion fully electric LMP3 car," 2022. [Online]. Available: https://www.inmotion.tue.nl/en/about-us/cars/revolution

[35] J. Löfberg, "YALMIP : A toolbox for modeling and optimization in MATLAB," in *IEEE Int. Symp. on Computer Aided Control Systems Design*, 2004.

[36] Mosek APS. The MOSEK optimization software. Available at http://www.mosek.com.

[37] A. J. Conejo, E. Castillo, R. Minguez, and R. Garcia-Bertrand, *Decomposition techniques in mathematical programming: engineering and science applications*. Springer Science & Business Media, 2006.